Int J Adv Manuf Technol (2018) 96:1625–1633
DOI 10.1007/s00170-017-0837-5

ORIGINAL ARTICLE

Microstructure and performance of multi-dimensional WC-CoCr coating sprayed by HVOF

Xiang Ding[1] · Xu-Dong Cheng[1] · Chao Li[2] · Xiang Yu[2] · Zhang-Xiong Ding[2] · Cheng-Qing Yuan[2]

Received: 14 December 2016 / Accepted: 18 July 2017 / Published online: 1 August 2017

Abstract WC-based coatings deposited by high velocity oxy-fuel (HVOF) spraying have been widely used in many industrial fields, where mechanical components are subjected to severe abrasive wear. Much attention has been especially paid to nanostructured and multimodal WC-based coatings due to their excellent abrasive wear resistance. In this study, a new kind of multi-dimensional WC-10Co4Cr coating, composed of nano, submicron, micron WC particles and CoCr alloy, was developed by HVOF. The microstructure, porosity, microhardness, fracture toughness, and electrochemical properties of the coating were investigated in comparison with nanostructured WC-10Co4Cr coating deposited by HVOF. Abrasive wear resistance of both WC-10Co4Cr coatings was evaluated on wet sand rubber wheel abrasion tester. The results show that the multi-dimensional coating possesses low porosity (0.31 ± 0.09%), excellent microhardness (1126 ± 115 $HV_{0.3}$), fracture toughness (4.66 ± 0.51 MPa $m^{1/2}$), and outstanding electrochemical properties. Moreover, the multi-dimensional coating demonstrates approximately 36% wet abrasive resistance enhancement than the nanostructured coating. The superior abrasive wear resistance originates from the coating's multi-dimensional structure and excellent mechanical and electrochemical properties.

✉ Chao Li
374443668@qq.com

Xiang Ding
dingxiang@whut.edu.cn

[1] State Key Laboratory of Advanced Technology for Materials and Processing, Wuhan University of Technology, Wuhan 430070, China

[2] School of Energy and Power Engineering, Wuhan University of Technology, Wuhan 430063, China

Keywords WC-CoCr coatings · High velocity oxy-fuel spray · Multi-dimensional · Microstructure · Performance

1 Introduction

Mechanical components in a number of industrial fields are subjected to severe abrasive wear, such as shipping, metallurgy, energy, and construction industry, and have become one of the most serious issues for equipment failure. Because wear only occurs on the surface of components, surface engineering techniques have become the most effective solutions for the wear problems [1–3]. For example, thermal spraying, plasma nitriding, chemical vapor deposition, physical vapor deposition, laser cladding, and hardening have been developed to improve the wear resistance of component surface. Among them, thermal spraying methods, including air plasma spraying (APS), detonation gun (D-Gun), and high velocity oxy-fuel spraying (HVOF), have been commercially employed on some machinery components [4–6].

WC-based coatings can offer a combination of high hardness and excellent toughness, in which high hardness comes from WC particles, whereas the binder matrix is responsible for excellent toughness in the cermet materials [7, 8]. Among various WC-based cermet coatings deposited by thermal spray techniques, WC-Co coatings, especially with nano-sized WC, have already been successfully applied in a wide range of wear-resistant machinery [9, 10]. Moreover, the addition of chromium to the cobalt binder can improve the corrosion resistance of WC-Co coatings and enhance the coatings' strength. Therefore, outstanding corrosion and wear resistance make WC-CoCr coating a promising candidate for applications where both corrosion and wear resistance are critical [11–13].

WC grain size is one of the most critical factors affecting the mechanical properties and wear performance of WC-based cermet coatings [14–16]. Some researchers suggest that adding fine WC particles into the coatings can enhance wear performance [17–21]. A number of researches have confirmed that the hardness and toughness of nanostructured coatings can simultaneously increase [22, 23]. However, the mechanism of the improved wear performance has been a controversial and much disputed subject [24, 25]. Several studies reveal that coating's fracture toughness is reduced as WC size decreases, caused by the formation of unwanted carbides (W_2C, complex Co-W-C, or even metallic W) owing to the decarburization of nano WC, which can lower the mechanical properties of nanostructured WC-based coatings [26–29]. In order to limit the extent of decarburization and reduce the high cost of nano WC-based coating, multi-dimensional WC-based coatings have been investigated by some researchers. Nevertheless, the WC-based coatings were actually deposited with bimodal WC-Co powders composed just of nano and micro WC [30–35] and a mixed multimodal WC-Co powder [36]. Using the mixed multimodal powder would lead to uneven microstructure. Also, it was found that decarburization still happens in some degree and the fracture toughness of coatings was below satisfying owe to high nano WC rate in the multimodal coatings. Therefore, it is difficult to achieve the ideal wear resistance of the multimodal WC-based materials. Furthermore, these publications all are about WC-Co coatings, and up to now, there are no reports about multi-dimensional WC-CoCr coatings deposited by thermal spraying.

The deposition process is another important factor to influence the structures and properties of WC-based cermet coatings. Most commonly applied thermal spraying processes to deposit the coatings include D-Gun, arc plasma (APS), and HVOF. In HVOF process, WC powder is accelerated at a high velocity (600–1200 m/s) and it provides sufficiently high coating adhesion (>70 MPa) to the substrate surface. As compared to D-Gun (~4000 °C) and APS (~7000 °C), HVOF results in less phase change due to lower flame temperature (~2700 °C) and also produces relatively denser coatings [37]. The characteristics of high velocity and moderate temperature of HVOF flame can hinder the decarburization of WC during spraying. Hence, HVOF is considered as an ideal method to prepare various WC-CoCr cermet coatings with nano-sized WC particles [13, 38].

In this study, a new multi-dimensional WC-CoCr cermet coating containing nano, submicro, and micro WC particles was deposited by HVOF. The design is expected to reduce the decarburization of nano-sized WC, simultaneously improve the hardness and toughness of the multi-dimensional coating, and enhance the wear performance. The structure, mechanical and electrochemical properties, and wet abrasive wear performance of the multi-dimensional WC-CoCr coating were investigated, compared with nanostructured WC-CoCr coating deposited by the same method. The study of wear mechanisms of the multi-dimensional coating can provide valuable insights into the design and application of WC-CoCr anti-abrasion coatings.

2 Experimental procedure

2.1 Coating materials

Multi-dimensional and nanostructured WC-10Co4Cr cermet composite powders containing nano-sized WC were used as feedstock (marked MP and NP, respectively) in the present study, which were manufactured by an agglomeration-

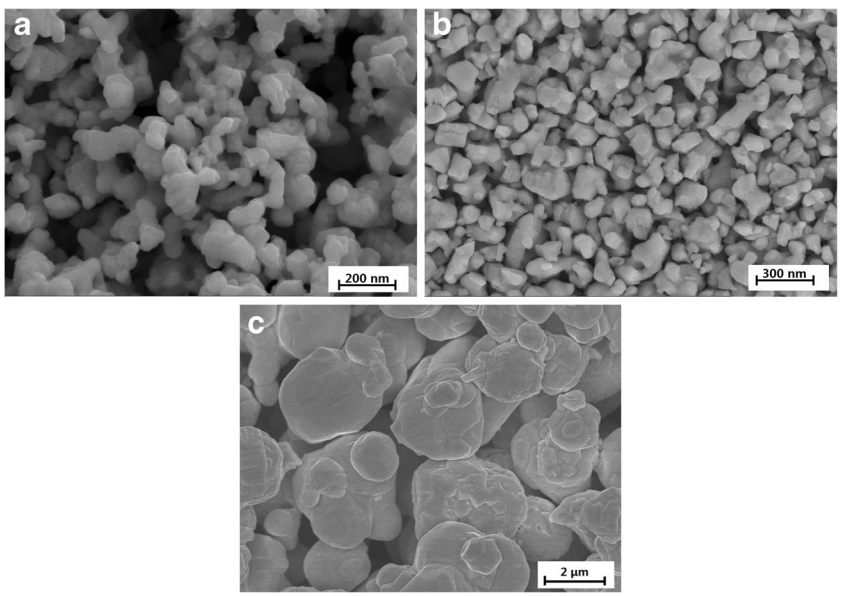

Fig. 1 SEM images of nano WC (**a**), submicro WC (**b**), and micro WC (**c**)

sintering method. In MP (T64T440, Achteck, China), the carbide is composed of 20 vol% nano WC (80 ~ 180 nm), 30 vol% submicron WC (0.4–0.6 μm), and 50 vol% micron WC (~2.5 μm). The morphology of nano, submicron, and micron WC particles are shown in Fig. 1. The fabrication of MP involved ball milling of a mixture of different sized WC particles, Co, Cr_3C_2, and several addictive, followed by spray drying and sintering. The size of MP is in the range of 20–53 μm, while the size of NP (S7410, Inframat, USA) distributes between 15 and 45 μm and WC grain size is 100–500 nm.

Figure 2 illustrates the SEM micrographs of two WC-10Co4Cr cermet powders. Both MP and NP are highly spherical (Fig. 2a, c). Meanwhile, different sized WC particles and some voids on the surface can be observed at high magnification (Fig. 2b, d). Nano, submicro, and micro WC particles are clearly observed in multi-dimensional powder (Fig. 2b), while nanostructured powder has nano-sized WC particles evenly distributed within it (Fig. 2d).

2.2 Coating deposition

The multi-dimensional and nanostructured WC-10Co4Cr coatings (marked as MC and NC, respectively) were deposited by JP8000 HVOF system (Praxair, USA) using kerosene as fuel and oxygen as oxidant gas. The parameter selection was based on velocity and temperature measurements made by a Spraywatch-2i diagnostic device (Oseir, Finland), and optimized parameters are listed in Table 1. The coatings were deposited on 304 stainless steel substrates, which were grit blasted with 60 mesh alumina particles at 0.55-MPa pressure followed by ultrasonic cleaning in acetone before spraying. During spraying, sufficient air cooling was applied and substrate temperature was controlled around 150 ± 30 °C. The final thickness of the coatings was ~450 ± 20 μm. All the samples were ground and polished to an average surface roughness Ra ≤ 0.02 μm before further coating characterization.

Table 1 Main spray parameters of WC-10Co4Cr coatings by HVOF

Coating no.	MC	NC
Powder type	MP	NP
Gun length (inch)	6	6
Fuel flow (GPH)	6.0	6.0
Oxygen flow (SCFH)	1950	2000
Powder feed rate (g/min)	75	75
Stand-off distance (mm)	380	380
Spraying velocity (mm/s)	500	500

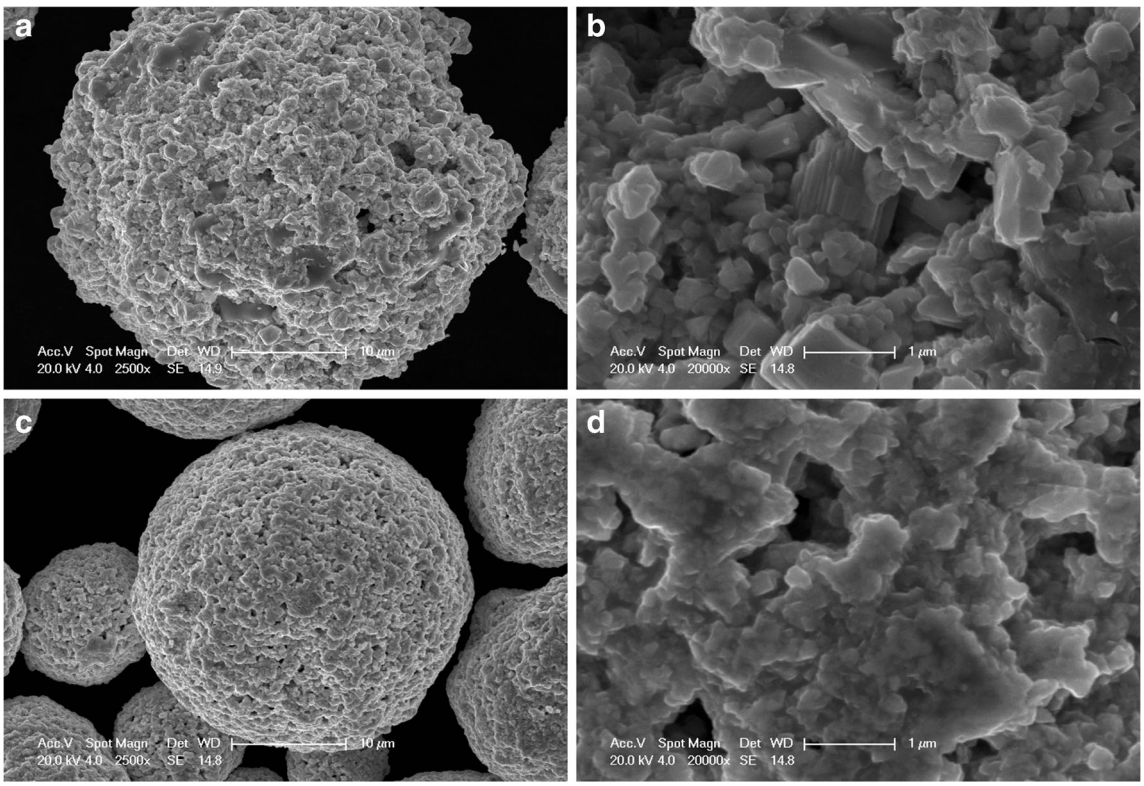

Fig. 2 Micrographs of WC-10Co4Cr powders with nano-sized WC at different magnification: MP (**a**, **b**) and NP (**c**, **d**)

2.3 Coating characterization

The morphology and microstructures of the coatings were observed with VHX-2000 digital optical microscope (OM), FEI Quanta 250 scanning election microscope (SEM) and JEM-2100F transmission electron microscopy (TEM). Phase identification for the powders and the coatings was carried out by a D/max-2550 diffraction meter (XRD) using Cu-K_α radiation with $\lambda = 0.154$ nm. Microhardness measurement of the coatings was performed on the cross section of coatings via HVS-1000 Vickers microhardness tester at the load of 300 g for a loading time of 15 s. The porosity was measured with metallographic 500× photos by Axiovet 40 MAT metallographic microscope, followed by porosity calculation using IQ materials software (the value was the average value of six points). The fracture toughness K_c was calculated according to the Wilshaw equation (1) [39] (the result was the average value of ten measurements), where P, a, and c are the load of Huayin HV5 type Vickers hardness meter (5 kg), half the length of indentation diagonal and half the length of the crack, respectively.

$$K_c = 0.079 \frac{P}{a^{3/2}} \log\left(\frac{4.5a}{c}\right) \quad (1)$$

Potentiodynamic polarization test was carried out to compare the corrosion resistance of two coatings. The tests were conducted via a CS300 electrochemical system on a three-electrode test cell, with the specimen as working electrode, a platinum wire as auxiliary electrode, and a saturated calomel electrode as reference electrode. Specimens were carefully encapsulated using epoxy resin, leaving surface of ~0.785 cm^2 exposed to 3.5 wt% NaCl aqueous solution with temperature of 25 ± 1 °C.

2.4 Abrasion test

In the abrasion test, a rubber wheel (Φ178 mm × 12.7 mm) was used to provide low stress level in wet conditions. The coated specimens of 57 × 25 × 6 mm dimensions were tested using MLS-225 wet sand rubber wheel abrasion tester (Fig. 3). Steel wheels were covered by vulcanized rubber and turn against testing specimens under a load of 100 N with speed of 240 rpm. Forty weight percent of 60 mesh silica was mixed into water as abrasive. Coatings' mass loss was measured after 3500-revolutions abrasion test using TG328 electric balance to evaluate the wear performance. The volume wear loss (ΔV) is calculated by $\Delta W/\rho$, where ΔW and ρ are mass loss (average value of three specimen tests) and coating density, respectively. For comparison, abrasive wear test of sprayed and fused NiCrBSi alloy coating by flame (Ni60A, 60HRC) with 1.2 mm thickness was also performed under the same test condition.

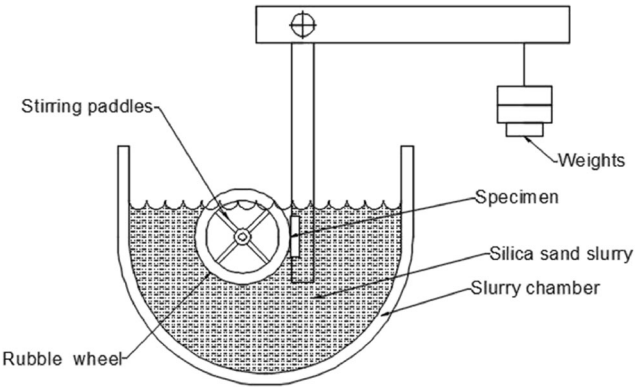

Fig. 3 Schematic diagram of the wear test apparatus

3 Results and discussion

3.1 Microstructures of WC-10Co4Cr coatings

Figure 4 represents the XRD patterns of two powders and corresponding coatings. It is shown that NP is mainly composed of WC, Co, and Co_3W_3C crystalline phases, but MP only consists of WC and Co phases. This is caused by different Cr element-adding methods during powder fabrication. Moreover, a small amount of W_2C phase is observed in addition to predominant WC phase in MC and BC coatings, but NC has a higher W_2C peak compared with MC, demonstrating more serious WC decarburization during spraying. The large specific surface area of nano WC particles can absorb heat from flame more easily for NC. Due to the small proportion of nano WC particles, the decarburization degree of multimodal coating is lower than nanostructured one. It is also observed that the Co_3W_3C and Co phases in the precursor powders leave no trace in both coatings, which can be explained by the pyrolysis and formation of Co-W-C amorphous structure during spraying, respectively [40, 41].

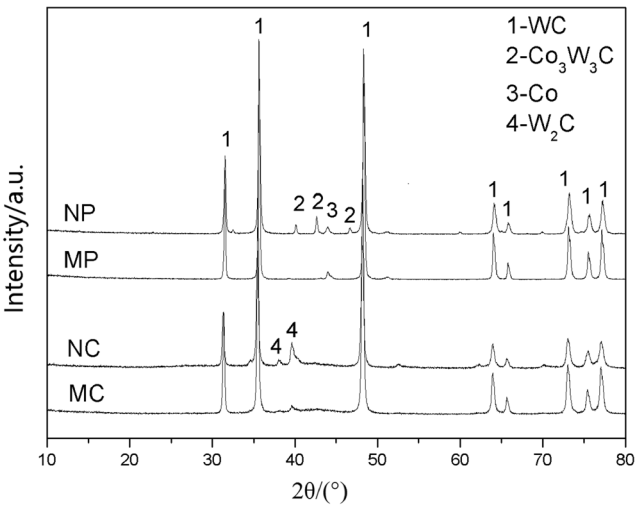

Fig. 4 XRD patterns of multi-dimensional and nanostructured WC-10Co4Cr powders and coatings

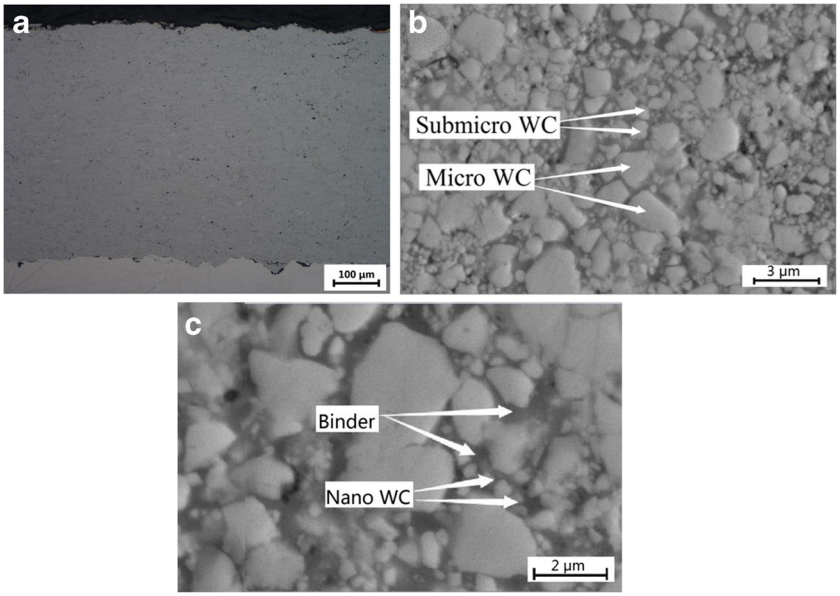

Fig. 5 Cross-sectional structures of the multi-dimensional WC-10Co4Cr coating at different magnification

The cross-sectional micrographs of the multi-dimensional WC-10Co4Cr coating are shown in Fig. 5. It can be observed from Fig. 5a that the microstructure of the multi-dimensional coating is dense, with porosity of 0.31 ± 0.09%. The pores generated between submicro and micro WC particles can be filled with dissolved nano WC and melted CoCr-binding phase. Furthermore, nanostructured coating demonstrates lower porosity (0.26 ± 0.05%) than multi-dimensional coating due to the better melting state obtained by dissolved larger proportion of nano WC particles.

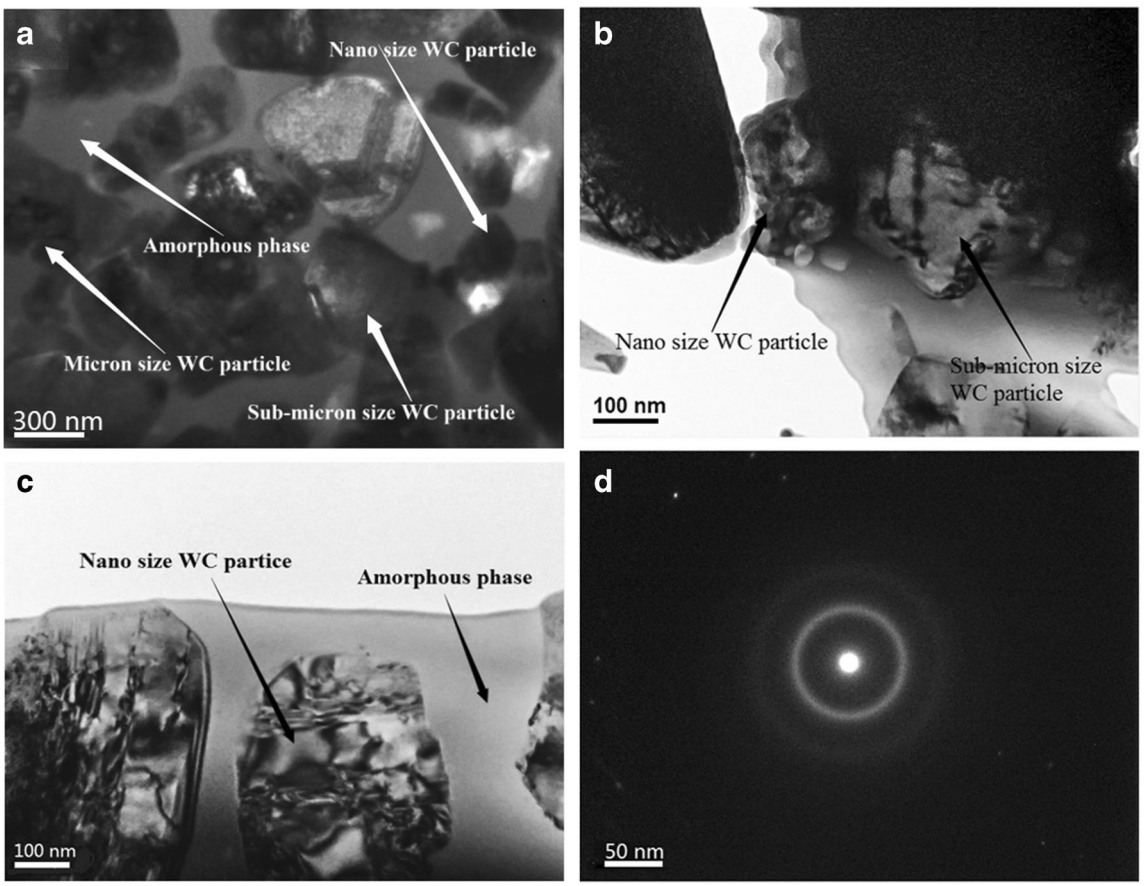

Fig. 6 TEM images of different sized WC and amorphous phases (**a**, **b**, **c**) and SAED pattern of amorphous phase (**d**) of the multi-dimensional WC-10Co4Cr coating

Table 2 Mechanical properties of WC-10Co4Cr coatings

Coatings	Microhardness ($HV_{0.3}$)	Fracture toughness (MPa $m^{1/2}$)
MC	1126 ± 64.3	4.66 ± 0.33
NC	1241 ± 86.0	4.16 ± 0.49

Table 3 Corrosion potentials and current densities of the coatings

Coatings	E_{corr} (V)	I_{corr} (μA cm^{-2})
MC	−0.31	3.12
NC	−0.42	3.22
Ni60A	−0.55	3.71

Nano-, submicron-, and micron-sized WC particles and binder in the multi-dimensional coating can be observed from Fig. 5b, c, and the microstructure is obviously different from the nanostructured coating deposited by HVOF reported by Hong S et al. and Thakur L and Arora N [13, 38]. The publications reveal that fine carbides are distributed uniformly in CoCr matrix and the pores exist in the nanosturctured WC-10Co4Cr coating. During the multi-dimensional WC-10Co4Cr powder deposition, CoCr alloy is the first material to melt, but among various sized WC, only the nano-sized WC particles can be dissolved into melted CoCr alloy, while the submicro and micro WC particles can merely reach semi-molten state. Thus, the melted Co-Cr-W-C particles fill into semi-molten submicro and micro WC particles, forming the micro-nano structure with the multi-dimensional WC particles. The dense multi-dimensional coating is expected to have high mechanical properties.

Figure 6a shows a typical bright field TEM image of multi-dimensional coating, which contains different sized WC phase and amorphous phase. Eighty-to-two-hundred-nanometer nano WC, 0.4–0.6-μm submicro WC particles, amorphous phase (indicated by arrows), and selected area electron diffraction (SAED) pattern of amorphous phase are further demonstrated from Fig. 6b–d, respectively. The diffraction pattern in Fig. 6d was taken with the selected area aperture centered over the amorphous region in Fig. 6c and shows a wide diffraction ring. The amorphous phase is caused by the rapid cooling of molten liquid CoCr alloy and dissolved nano WC particle, and the result is consistent with XRD analysis of the multi-dimensional WC-10Co4Cr coating.

3.2 Mechanical properties

Mechanical properties of two coatings sprayed by HVOF, including microhardness and fracture toughness, are shown in Table 2. Both coatings have microhardness values higher than 1100 $HV_{0.3}$. As nanostructured coating contains nano-sized WC and some high hard and brittle W_2C formed during the coating deposition, the coating possesses higher microhardness and lower fracture toughness. Meanwhile, multi-dimensional coating obtains the fracture toughness of ~4.66 MPa $m^{1/2}$, which is 12% higher than that of nanostructured coating.

3.3 Electrochemical properties

The potentiodynamic polarization curves of MC, NC, and Ni60A coatings in 3.5 wt% NaCl aqueous solution are shown in Fig. 7. The corresponding electrochemical values are listed in Table 3. The corrosion potentials (E_{corr}) of the MC, NC, and Ni60A coatings are about −0.31, −0.42, and −0.55 V, respectively. The corrosion current density (I_{corr}) of MC and NC coatings are 3.12 and 3.22 μA cm^{-2}, which are obviously smaller than that of the Ni60A coating (3.71 μA cm^{-2}).

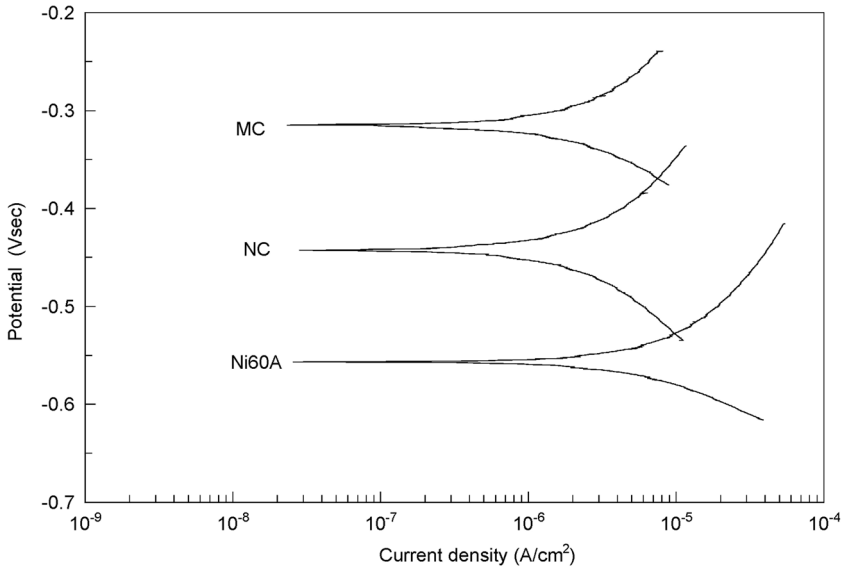

Fig. 7 Tafel plots of Ni60A and WC-10Co4Cr coatings

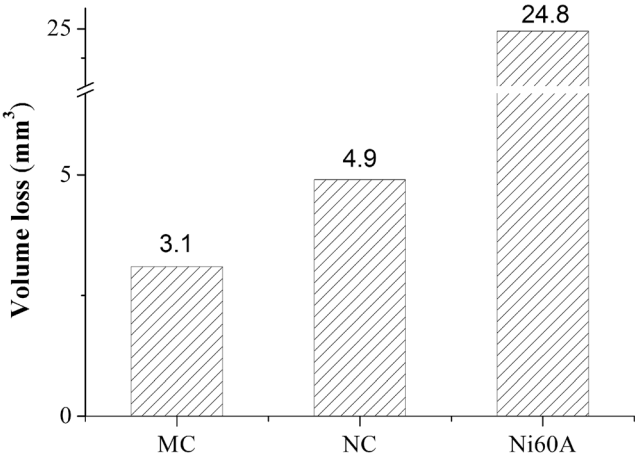

Fig. 8 Abrasive wear volume loss of different coatings

Furthermore, multi-dimensional WC-10Co4Cr coating exhibits superior corrosion resistance compared to the nanostructured coating, which can be attributed to its dense and multi-dimensional microstructure with no obvious W_2C.

3.4 Abrasion performance and mechanisms

The abrasive wear volume losses of HVOF-sprayed WC-10Co4Cr coatings and Ni60A coating are presented in Fig. 8. It is shown MC demonstrates the best abrasive resistance. In comparison with the Ni60A coating, the abrasive wear resistance of WC-10Co4Cr coatings has been enhanced more than 4.0 and 7.0 times, respectively, and the abrasive wear resistance of the multi-dimensional coating is obviously higher than that of the nanostructured coating.

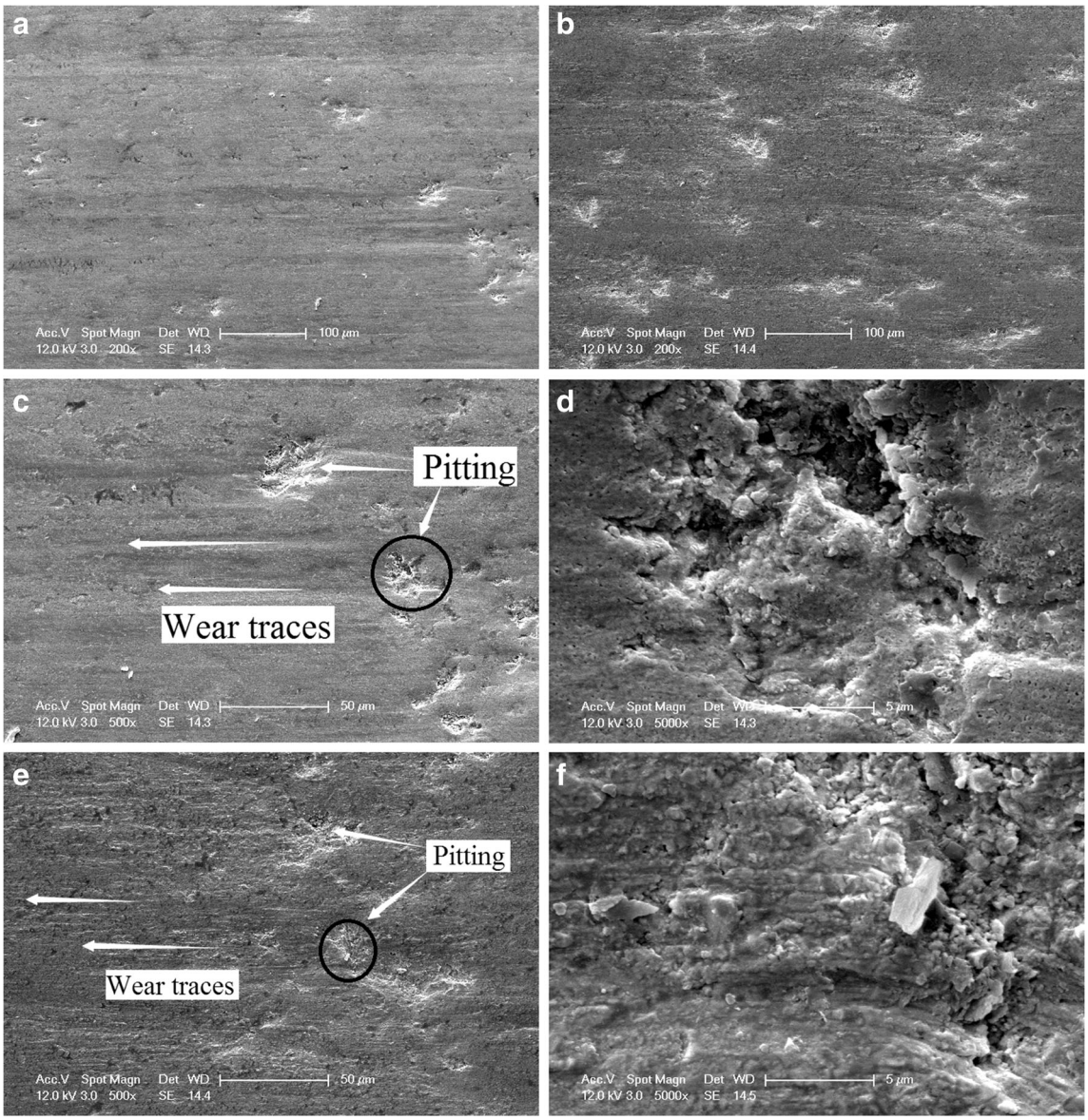

Fig. 9 Abrasive wear surface micrographs of multi-dimensional (**a**, **c**, **d**) and nanostructured (**b**, **e**, **f**) coatings

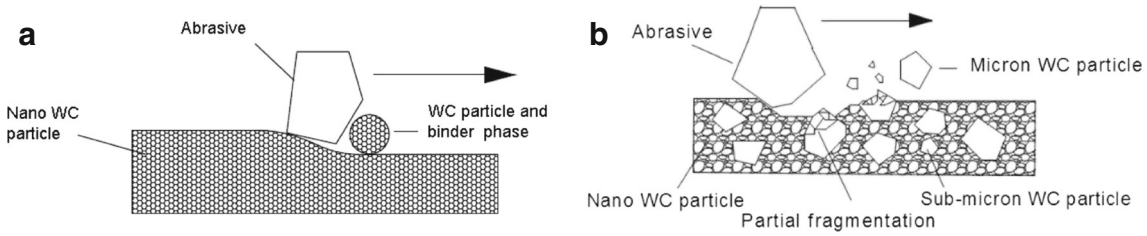

Fig. 10 Abrasion wear schematic diagram of two coatings

The abraded surface micrographs of WC-10Co4Cr coatings are illustrated in Fig. 9. Pitting and long furrow wear traces can be clearly observed on the surface of the two coatings. The abraded surface features of the two coatings are similar, and the wear traces almost originate from the pitting, but the wear degree of nanostructured coating is more serious than multi-dimensional one. In the process of abrasive wear, when sand particles move across the contact surface between soft rubber wheel and hard coating, most of particles are gripped by the rubber wheel due to limited penetration of particles to the hard surface. Therefore, only the corner of abrasive particles will embed the surface of coating. Most material losses of nanostructured coating are from shallow micro-plowing, leading to the removal of binder and nano WC grains along with it, as shown in Fig.10a. Since the multi-dimensional coating possesses lower hardness, the corner of abrasive penetrates more deeply. However, its multi-dimensional structure can obstruct abrasive micro-plowing on the surface. In multi-dimensional coatings, the micron WC particles bury deeply in binding phase and are more difficult to detach than small ones, resulting in shallow-abraded scratches.

From Fig. 9d, f, it can be observed that nano WC particles and binder phase are cut along wear trace as abrasive plows across the surface of nanostructured coatings. On the other hand, the wear mechanism of multi-dimensional coating is partial fragmentation and particle detachment in the form of pitting; then, abrasive generates scratches in the subsequent path, as shown in Fig.10b. The different abrasion mechanisms of multi-dimensional and nanostructured WC-10Co4Cr coatings originate from the different structure. In multi-dimensional coatings, micron WC particles can protect the CoCr binder phase and fine WC particles from micro-plowing at the subsequent cutting path. However, the nanostructured coating without multi-dimensional WC structure lacks such protection mechanism.

From the above analysis, it is known that nanostructured WC-10Co4Cr coating has more complex phase composition with higher content of W_2C. Because W_2C, WC, and CoCr alloys have different corrosion potentials, electrochemical corrosion will occur between different phases in aqueous solution and tiny corrosion pits will form. Therefore, the bonding force between different particles is reduced. On the other hand, W_2C in nanostructured coating will increase the brittleness of the coating. During the wear process, the corrosion pits and brittleness lead to the formation of micro cracks on the coating surface, making the particles on the coating surface more easily fall off. Thus, these features of nanostructured coating further reduce coating's wear resistance.

4 Conclusions

Following conclusions can be reached by this research:

(1) In multi-dimensional WC-10Co4Cr coating deposited by HVOF, carbides mainly consist of WC with no obvious WC decarburization.
(2) Compared with the nanostructured WC-10Co4Cr coating, multi-dimensional coating exhibits 12% higher fracture toughness than that of the nanostructured one.
(3) The multi-dimensional WC-10Co4Cr coating possesses more excellent electrochemical properties than the nanostructured one.
(4) The multi-dimensional WC-10Co4Cr coating demonstrates most outstanding abrasive wear resistance. The excellent wet abrasive resistance, which is enhanced approximately 36% than the nanostructured coating, originates from the coating's multi-dimensional structure that leads to excellent mechanical and electrochemical properties.

Acknowledgements This research was supported by the National Natural Science Foundation of China under the project (51422507).

References

1. Kamdi Z, Shipwaya PH, Voiseya KT, Sturgeon AJ (2011) Abrasive wear behavior of conventional and large-particle tungsten carbide-based cermet coatings as a function of abrasive size and type. Wear 271:1264–1272
2. Wang Q, Chen ZH, Ding ZX (2009) Performance of abrasive wear of WC-12Co coatings sprayed by HVOF. Tribol Int 42:1046–1051

3. Stewart DA, Shipway PH, and McCartney DG (1999) Abrasive wear behaviour of conventional and nanocomposite HVOF sprayed WC-Co coatings. Wear 225–229:789–798
4. Singh R, Tiwari SK, Mishra SK (2012) Cavitation erosion in hydraulic turbine components and mitigation by coatings: current status and future needs. J Mater Eng Perform 21(7):1539–1551
5. Shipway PH, McCartney DG, Sudaprasert T (2005) Sliding wear behavior of conventional and nanostructured HVOF sprayed WC/Co coatings. Wear 259:820–827
6. Jafarzadeh K, Valefi Z, Ghavidel B (2010) The effect of plasma spray parameters on the cavitation erosion of Al_2O_3-TiO_2 coatings. Surf Coat Technol 205(7):1850–1855
7. Hong S, Wu YP, Zhang JF, Zheng YG, Zheng Y, Lin JR (2016) Synergistic effect of ultrasonic cavitation erosion and corrosion of WC-CoCr and FeCrSiBMn coatings prepared by HVOF spraying. Ultrason Sonochem 31:563–569
8. Wang Q, Tang ZX, Cha LM (2015) Cavitation and sand slurry erosion resistances of WC-10Co-4Cr coatings. J Mater Eng Perform 24(6):2435–2443
9. Kim HJ, Yang HS, Baik KH (2006) Development and properties of nanostructured thermal spray coatings. Curr Appl Phys 6(6):1002–1006
10. Tillmann W, Baumann I, Hollingsworth PS et al (2014) Sliding and rolling wear behavior of HVOF-sprayed coatings derived from conventional, fine and nanostructured WC-12Co powders. J Therm Spray Technol 23(1/2):262–280
11. Zhou KS, Deng CM, Liu M (2009) Characterizations of fatigue and salt spray corrosion resistance of HVAF sprayed WC-17Co and WC-10Co4Cr coatings on the substrate of 300M steel. Rare Metal Mat Eng 38(4):671–676
12. Hong S, Wu YP, Zhang JF (2015) Cavitation erosion behavior and mechanism of HVOF sprayed WC-10Co-4Cr coating in 3.5 wt% NaCl solution. Trans Indian Inst Metals 68(1):151–159
13. Hong S, Wu YP, Zhang JF (2015) Ultrasonic cavitation erosion of high-velocity oxygen-fuel (HVOF) sprayed near-nanostructured WC-10Co-4Cr coating in NaCl solution. Ultrason Sonochem 26:87–92
14. Ghabchi A, Varis T, Turunen E, Suhonen T, Liu XW, Hannula SP (2010) Behavior of HVOF WC-10Co4Cr coatings with different carbide size in fine and coarse particle abrasion. J Therm Spray Technol 19(1–2):368–377
15. Armstrong RW (2011) The hardness and strength properties of WC-Co composites. Materials 4(7):1287–1308
16. Ma N, Guo L, Cheng ZX, Wu HT, Ye FX, Zhang KK (2014) Improvement on mechanical properties and wear resistance of HVOF sprayed WC-12Co coatings by optimizing feedstock structure. Appl Surf Sci 320:364–371
17. Jia K, Fischer TE (1996) Abrasion resistance of nanostructured and conventional cemented carbides. Wear 200:206–214
18. Li CJ, Ohmori A, Tani K (1999) Effect of WC particle on the abrasive wear of thermally sprayed WC-Co coatings. Mater Manuf Process 14:175–184
19. Scieska SF, Filipowicz K (1998) An integrated testing method for cermet abrasion resistance and fracture toughness evaluation. Wear 216:202–212
20. Gee MG, Gant A, Roebuck B (2007) Wear mechanism in abrasion and erosion of WC/Co and related materials. Wear 263:137–148
21. Guilemany JM, Dosta S, Miguel JR (2006) The enhancement of the properties of WC–Co HVOF coatings through the use of nanostructured and microstructured feedstock powders. Surf Coat Technol 201:1180–1190
22. Zhao XQ, Zhou HD, Chen JM (2006) Comparative study of the friction and wear behavior of plasma sprayed conventional and nanostructured WC-12%Co coatings on stainless steel. Mater Sci Eng 431(1–2):290–297
23. Chen H, Gou GQ, Tu MJ (2009) Characteristics of nano particles and their effect on the formation of nanostructures in air plasma spraying WC-17Co coating. Surf Coat Technol 203(13):1785–1789
24. Shipway PH, Hogg JJ (2005) Dependence of microscale abrasion mechanisms of WC-Co hard metals on abrasive type. Wear 259(1–6):44–51
25. He J, Liu Y, Qiao Y, Fischer TE, Lavernia EJ (2002) Near-nanostructured WC-18 pct Co coatings with low amounts of non-WC carbide phase: part I. Synthesis and characterization. Metall Mater Trans A 33(1):145–157
26. Stewart DA, Shipway PH, McCartney DG (2000) Microstructural evolution in thermally sprayed WC-Co coatings: compassion between nanocomposite and conventional starting powders. Acta Mater 48:1593–1604
27. Babua PS, Basub B, Sundararajan G (2010) Abrasive wear behavior of detonation sprayed WC-12Co coatings: influence of decarburization and abrasive characteristics. Wear 268:1387–1399
28. Dent AH, DePaloand S, Sampath S, Therm J (2002) Examination of the wear properties of HVOF sprayed nanostructured and conventional WC-Co cermets with different binder phase contents. Spray Technol 11:551–558
29. Yang QQ, Senda T, Ohmori A (2003) Effect of carbide grain size on microstructure and sliding wear behavior of HVOF-sprayed WC-12%Co coatings. Wear 254:23–34
30. Skandan G, Yao R, Sadangi R (2000) Multimodal coatings: a new concept in thermal spraying. J Therm Spray Technol 9(3):329–331
31. Gang CJ, Hong TW, Xiao C et al (2013) Characterization of cold-sprayed multimodal WC-12Co coating. Surf Coat Technol 235: 536–543
32. Wang Q, Chen ZH, Lia LX, Yang GB (2012) The parameters optimization and abrasion wear mechanism of liquid fuel HVOF sprayed bimodal WC-12Co coating. Surf Coat Technol 206: 2233–2241
33. Ding ZX, Chen W, Wang Q (2011) Resistance of cavitation erosion of multimodal WC-12Co coatings sprayed by HVOF. Trans Nonferrous Met Soc China 21:2231–2236
34. Skandan G, Yao R, Kear BH, Qiao Y, Liu L, Fischer TE (2001) Multimodal powders: a new class of feedstock material for thermal spraying of hard coatings. Scripta Mater 44:1699–1702
35. Ma N, Guo L, Chen ZX, Wu H, Ye F, Zhang K (2014) Improvement on mechanical properties and wear resistance of HVOF sprayed WC-12Co coatings by optimizing feedstock structure. Appl Surf Sci 320:364–371
36. Wang HT, Chen X, Bai XB, Ji GC, Dong ZX, Yi DL (2014) Microstructure and properties of cold sprayed multimodal WC-17Co deposits. Int J Refract Met Hard Mater 45:196–203
37. Toma D, Brandl W, Marginean G (2001) Wear and corrosion behaviour of thermally sprayed cermet coatings. Surf Coat Technol 138:149–158
38. Thakur L, Arora N (2013) A study on erosive wear behavior of HVOF sprayed nanostructured WC-CoCr coatings. J Mar Sci Technol 27(5):1461–1467
39. Sahraoui T, Guessasma S, Jeridane ML et al (2010) HVOF sprayed WC-Co coatings: microstructure, mechanical properties and friction moment prediction. Mater Des 31:1431–1437
40. Lekatou A, Sioulas D, Karantzalis AE, Grimanelis D (2015) A comparative study on the microstructure and surface property evaluation of coatings produced from nanostructured and conventional WC-Co powders HVOF-sprayed on Al7075. Surf Coat Technol 276:539–556
41. Sugiyama K, Nakahama S, Hattori S, Nakano K (2005) Slurry wear and cavitation erosion of thermal-sprayed cermets. Wear 258(5–6): 768–775